Journal of Physics: Conference Series **427** (2013) 012009 doi:10.1088/1742-6596/427/1/012009

Self-consistent Green's functions calculation of the nucleon mean-free path

A. Rios[1] **and V. Somà**[2,3]

[1] Department of Physics, Faculty of Engineering and Physical Sciences, University of Surrey, Guildford, Surrey GU2 7XH, United Kingdom
[2] Institut für Kernphysik, Technische Universität Darmstadt, 64289 Darmstadt, Germany
[3] ExtreMe Matter Institute EMMI, GSI Helmholtzzentrum fur Schwerionenforschung GmbH, 64291 Darmstadt, Germany

E-mail: a.rios@surrey.ac.uk

Abstract. Transport coefficients provide a unique insight into the near-equilibrium behavior of quantum many-body systems. The mean-free path, λ, of a particle within a dense medium is a basic transport coefficient, at the basis of several theoretical concepts and closely related to experimentally measured quantities. Green's functions techniques are particularly well suited to study such transport properties, since they are naturally formulated in the time domain. We present a calculation of the mean-free path of a nucleon in symmetric nuclear matter using self-consistent ladder self-energies extended to the complex energy plane. Our results indicate that, for energies above 50 MeV at densities close to saturation, a nucleon has a mean-free path of 4 to 5 femtometers.

1. Introduction

Over the years, the nuclear many-body community has primarily concentrated on the study of the equilibrium properties of extended hadronic systems [1]. A focal point of these efforts has been the calculation of the Equation of State (EoS) of neutron matter [2]. This determines to a large extent the mass-radius relation of neutron stars, which is expected to be experimentally constrained by near-future astronomical observations. The hope is that precise simultaneous measurements of both the radius and the mass of pulsars will indirectly provide precious information on nucleon-nucleon interactions and more in general on strongly interacting nuclear systems [3, 4].

Transport properties characterize the behaviour of systems when driven out of equilibrium [5]. Viscosities and mean-free paths determine the dynamics of damping (or potential growth) of various instability modes and give insight on the microscopic structure of the medium. Unlike those of equilibrium properties, calculations of transport coefficients of homogeneous hadronic matter are relatively scarce. These coefficients, however, are extremely important to describe the dynamics and time evolution of astrophysical compact objects and affect the analysis of present generation astronomical observations. The rapid cooling observed in Cassiopeia A, for instance, is thought to be related to a modification in the specific heat associated to pairing phenomena [6] and it is sensitive to transport in dense matter [7, 6]. Shear and bulk viscosities are often needed in neutron star modeling [8, 9, 10]. In particular, the potential instability to general relativistic modes is very sensitive to the bulk viscosity [11].

In some cases, the theoretical calculations of transport coefficients involve an artificial coupling between the many-body treatment (or the equilibrium problem) and the transport (or non-equilibrium) approach. A typical example is provided by recent calculations of the shear viscosity [10, 12]. The equilibrium problem is treated using many-body techniques, like the Correlated Basis Functions or the Brueckner-Hartree-Fock approaches. These provide access to scattering properties in equilibrated dense matter, in particular in-medium cross sections. The latter can then be used as input in an Abrikosov-Khalatnikov-type calculation for the viscosity [13]. Yet, the scattering processes described by equilibrium many-body calculations need not be the same as those originally considered within Abrikosov theory. One can therefore argue that, by coupling both approaches, uncontrolled errors are being introduced in the calculation.

In contrast, Green's functions are well suited to compute transport coefficients from first principles. Time dependence is treated explicitly in the theory [14], to the extent that one can even consider non-equilibrium dynamics in a meaningful way [15]. Pauli principle and beyond mean-field correlations can be consistently taken into account. Kubo relations give access to several non-equilibrium properties from correlators computed near equilibrium [16] and have been used to compute a handful of transport coefficients in a wide variety of systems [17]. In principle, two-time Kadanoff-Baym calculations could also provide reliable calculations of transport properties beyond the near-equilibrium assumption. In the following, we concentrate on the application of equilibrium Green's functions techniques to compute the mean-free path of particles in the nuclear medium.

2. Nucleon mean-free path

The mean-free path, λ, is perhaps the best studied transport coefficient in nuclear physics, as it is directly linked to the medium's absorptive properties [18, 19, 20, 21, 22]. This absorption is closely related to nuclear optical potentials, which can be fitted or measured in a variety of experiments. In the past, the lack of microscopic propagators in nuclear systems has hampered the calculation of transport coefficients using Green's function techniques. Consequently, most previous attempts to compute the mean-free path have been derived from extensions of Brueckner's theory of nuclear matter [18, 19, 21, 23, 24, 25]. These calculations have been performed at energies arbitrarily close to the real axis and, as a consequence, ad-hoc non-locality corrections have had to be introduced, generally through the $k-$mass approximation [18].

Our philosophy has been that of a fully *ab initio* calculations and we have sought to introduce as few approximations as possible. Our starting point are state-of-the-art self-energies, computed within the ladder approximation both at zero and finite temperature [26, 27]. We take into account the underlying model dependence associated to different nucleon-nucleon (NN) interactions. We shall also briefly comment on the dependence on temperature and density of our results. As we shall see in the following, the extension of Green's functions techniques to the complex energy domain provides a consistent approach to compute quasi-particle (qp) properties [28, 18, 14]. Direct calculations on the complex energy plane have been performed in electronic systems since the early 1960's [29] and have been recently employed to describe microscopic excitations in solid state applications [30, 31]. To our knowledge, this represents the first application of these techniques within nuclear physics.

Our many-body approximation of choice is the *ladder approximation* implemented self-consistently [15]. Its formal and computational implementation is a demanding task and the interested reader can find more details in Refs. [32, 27]. Here, we summarise briefly the different stages of the approach. First, an energy- and momentum-dependent in-medium interaction, or $T-$matrix, is obtained from a Lippman-Schwinger equation, which succinctly reads:

$$T = V + VG_{II}T\,. \tag{1}$$

The in-medium two-body propagator, G_{II}, is a convolution of fragmented one-body propagators,

$\mathcal{G}(k,\omega)$, which naturally takes into account intermediate particle-particle and hole-hole states [33]. Further, the self-energy, $\Sigma(k,\omega)$, is obtained from the $T-$matrix by closing a fermionic line. The Dyson equation can then be used to find the in-medium propagator, $\mathcal{G}$. This gives rise to a self-consistent problem, as G_{II} depends on $\mathcal{G}$. For a given density and temperature, these equations are solved in an iterative fashion, taking into account the full energy and momentum dependence of all quantities. Three-body forces (3BF), which are necessary in nuclear systems, are included effectively via an average over a third, correlated nucleon [27].

2.1. Complex energy self-energy

The propagation of an excitation in nuclear matter is described by the retarded propagator, $\mathcal{G}_R(k,t) \equiv \Theta(t)\left\langle\left\{a(k,t),a^\dagger(k,0)\right\}\right\rangle$. In a uniform system in thermal equilibrium, $\mathcal{G}_R$ only depends on the time difference, t, and the momentum modulus, k. For a system with well-defined quasi-particles, the retarded one-body Green's functions has the following long-time asymptotic form [14, 34]:

$$\mathcal{G}_R(k,t) \xrightarrow[t>>\Gamma^{-1}]{} -i\,\eta(k)e^{-i\varepsilon(k)t}e^{-|\Gamma(k)|t}\,. \tag{2}$$

While $\eta(k)$ represents the strength of the excitation, the qp spectrum $\varepsilon(k)$ determines the oscillation frequency of the propagator. The spectrum is closely related to the group velocity,

$$v(k) = \frac{\partial\varepsilon(k)}{\partial k} = \frac{k}{m^*(k)}\,, \tag{3}$$

which is often studied in terms of an effective mass, $m^*(k)$. The inverse lifetime, $\Gamma(k)$, determines the timescale of the quasi-particle decay. Within Fermi liquid theory, one expects $\Gamma(k)$ to vanish near the Fermi surface. The knowledge of both the group velocity and the inverse lifetime is enough to compute the mean-free path through the fundamental relation:

$$\lambda(k) = \frac{v(k)}{|\Gamma(k)|}\,. \tag{4}$$

The question is how to extract both $\varepsilon(k)$ and $\Gamma(k)$ from the retarded propagator, $\mathcal{G}_R(k,\omega)$. Note that, in nuclear physics, the latter is traditionally computed in real time rather than in, say, Matsubara space [33]. From a Fourier transform point of view, one is tempted to associate Eq. (2) to a pole of order 1 in the lower half-plane [14]. The argument goes as follows. To Fourier transform to time-space, one integrates the propagator slightly above the real axis. If this contour is swapped to a contour that includes the (so-far hypothetical) pole in the lower complex plane, Cauchy's theorem guarantees the final result:

$$\mathcal{G}_R(k,t) = \int_{-\infty}^{\infty}\frac{\mathrm{d}\omega}{2\pi}\,e^{-i\omega t}\mathcal{G}(k,\omega_+) \sim \int_{C'}\frac{\mathrm{d}z}{2\pi}e^{-izt}\frac{\eta(z)}{z-(\varepsilon(k)-i|\Gamma(k)|)} = -i\eta(k)e^{-i\varepsilon(k)t}e^{-|\Gamma(k)|t}\,, \tag{5}$$

where $\omega_+ \equiv \omega + i\eta$ with $\eta \to 0$. The single pole description is particularly attractive due to its simplicity and its relation to Fermi liquid theory [35].

This description, however, is somewhat at odds with the complex extension derived from the Lehmann representation,

$$\mathcal{G}_R(k,\omega) = \int\frac{\mathrm{d}\omega'}{2\pi}\frac{\mathcal{A}(k,\omega')}{\omega_+-\omega'}\,. \tag{6}$$

The extension to the complex energy plane is obtained by replacing ω_+ with a complex energy, z. Such extension exists and is unique, but gives rise to a complex variable function that is analytic off the real axis [36]. In other words, the extension of $\mathcal{G}$ to complex energies implies that no poles are present in the complex plane. An illustration of the complex energy dependence of the propagator is given in the left panel of Fig. 1. This shows the imaginary part of $\mathcal{G}(k=0,z)$ for a SCGF self-energy obtained from a CDBonn NN interaction. The cut of $\mathcal{G}$ across the real axis is determined by the spectral function, $\mathrm{Im}\left\{\mathcal{G}(k,\omega_-)-\mathcal{G}(k,\omega_+)\right\}=\mathcal{A}(k,\omega)$. As expected, this extension to the complex plane does not yield a pole.

To recover Eq. (2) from the real frequency Fourier transform, we supposed that one could deform the integration contour from slightly above the real axis to just include the pole in the lower half-plane. The discontinuity of $\mathcal{G}$ across the real axis, however, precludes us from doing so. Instead, one could eliminate the discontinuity by providing a functional continuation, $\tilde{\mathcal{G}}$, which is continuous across the real axis. This continuation will have a pole in the lower half-plane. It is this pole, *i.e.* that of$\tilde{G}$ rather than that of $\mathcal{G}$, that can be associated to a qp.

The propagator in the complex energy plane fulfills a Dyson equation:

$$\mathcal{G}(k,z)=\frac{1}{z-\frac{k^2}{2m}-\Sigma(k,z)}\,, \tag{7}$$

with a self-energy, Σ, extended to complex energies in analogy with the complex extension of the propagator:

$$\Sigma(k,z)\equiv\int\frac{\mathrm{d}\omega}{2\pi}\frac{\gamma(k,\omega)}{z-\omega}\,. \tag{8}$$

The function $\gamma(k,\omega)$ is proportional to the imaginary part of the self-energy near the real axis. The complex plane self-energy has the same analytic structure as the propagator, *i.e.* it is an analytic function except for the real axis. A way to obtain $\tilde{\mathcal{G}}$, is to use the complex Dyson equation, Eq. (7), with Σ replaced by the following extrapolation of the self-energy into the lower half-plane, $\tilde{\Sigma}$:

$$\tilde{\Sigma}(k,z)\equiv\begin{cases}\Sigma(k,z), & \mathrm{Im}\ z>0\\ \Sigma^*(k,z), & \mathrm{Im}\ z\leq 0\end{cases}\,. \tag{9}$$

This choice eliminates the discontinuity of Σ across the real energy axis and produces a pole in the lower half-plane propagator. This procedure seems to be valid in the case of the retarded propagator in nuclear matter, but one cannot exclude a different outcome in other cases.

The right plot in Fig. 1 shows the imaginary part of $\tilde{\mathcal{G}}(k=0,z)$. $\tilde{\mathcal{G}}$ is analytic across the real axis, but develops an isolated pole in the lower half-plane. The position of this pole is given by a zero in the denominator of the complex propagator, Eq. (7). This gives rise to the complex equation:

$$z(k)=\frac{k^2}{2m}+\mathrm{Re}\tilde{\Sigma}(k,z(k))+i\mathrm{Im}\ \tilde{\Sigma}(k,z(k))\,. \tag{10}$$

The solution, $z(k)=\varepsilon(k)+i\Gamma(k)$, yields the *fully dressed* qp spectrum and inverse lifetime. As we have access to the SCGF self-energies in the complex plane via Eq. (8), we are able to compute numerically the dressed spectra and lifetimes for different momenta, densities and temperatures. Note that, in the most general case, the solution to the previous equation need not be unique. We have not found any signature of multiple solutions in our nuclear matter calculations.

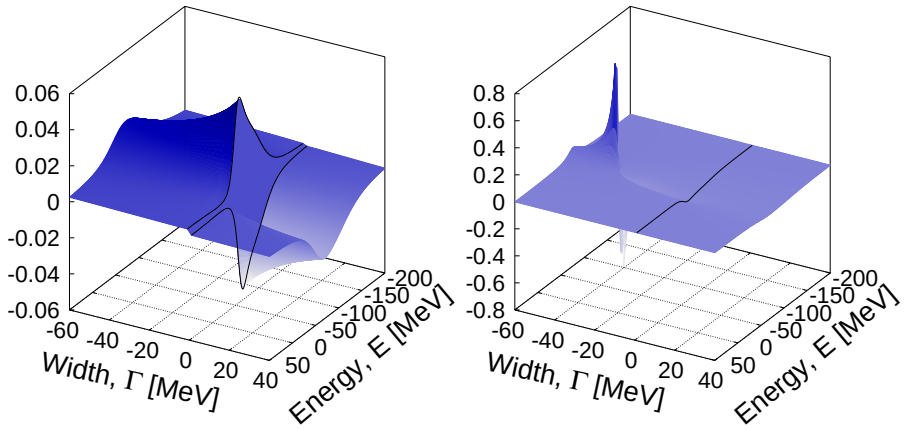

Figure 1. Imaginary part of the propagator in the complex energy plane, $z = E + i\Gamma$, at zero momentum for a CDBonn self-energy at $\rho = 0.16$ fm^{-3} and $T = 5$ MeV. The left plot corresponds to the usual propagator, $\mathcal{G}(k, z)$, while the right plot represents $\tilde{\mathcal{G}}(k, z)$. Solid lines show the imaginary part of the propagator just above/below the real axis, $\pm\mathcal{A}(k, \omega)/2$.

Our strategy can therefore be divided in four steps. First, we perform a ladder SCGF calculation of the self-energy along the real axis. We then extend the self-energy to the complex plane using its Lehmann representation, Eq. (9). The knowledge of $\Sigma(k, z)$ in the upper half plane is then used to find $\tilde{\Sigma}$ in the lower half-plane. Finally, using Eq. (10), one can determine the qp properties and hence the mean-free path. In the next section, we will discuss the result of these calculations for symmetric nuclear matter.

2.2. Other approaches

Previous calculations have relied on solving Eq. (10) using successive approximations for the dependence on the imaginary part of the complex energy of $\tilde{\Sigma}$ [18, 19, 21]. In the following, the different orders in the approximation are referred to as *renormalizations*, in accordance to the usual solid state nomenclature [31]. At the lowest order, known as *first renormalization*, one completely neglects the dependence on the imaginary part of z. This provides the usual definition of a qp:

$$\varepsilon_1(k) = \frac{k^2}{2m} + \mathrm{Re}\tilde{\Sigma}(k, \varepsilon_1(k))\,, \tag{11}$$

$$\Gamma_1(k) = \mathrm{Im}\ \tilde{\Sigma}(k, \varepsilon_1(k))\,, \tag{12}$$

which coincides with the peak of the spectral function. A *second renormalization* qp pole is obtained by expanding the self-energy around $z_1(k)$ to first order in the imaginary part of z,

$$\varepsilon_2(k) = \varepsilon_1(k) - \mathrm{Im}\ \tilde{\Sigma}(k, \varepsilon_1(k))\,\mathrm{Im}\ \frac{1}{1 - \tilde{\Sigma}'(z_1(k))}\,, \tag{13}$$

$$\Gamma_2(k) = \Gamma_1(k)\,\mathrm{Re}\frac{1}{1 - \tilde{\Sigma}'(z_1(k))}\,. \tag{14}$$

In the context of nuclear physics, it has generally been assumed that the dependence of $\tilde{\Sigma}$ on the imaginary part of z is soft and can be ignored in the previous derivatives [18]. This gives

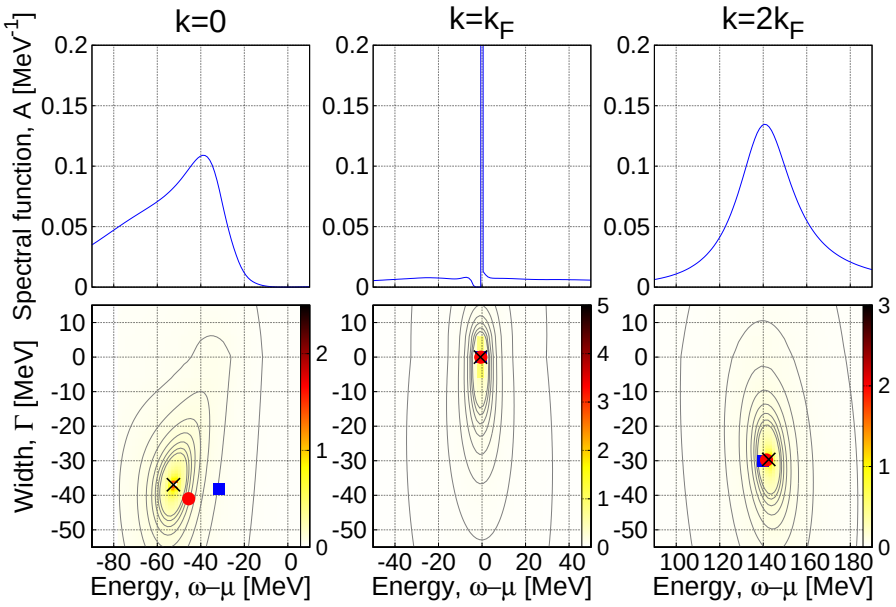

Figure 2. Upper panels: spectral function at $\rho = 0.16$ fm^{-3} and $T = 0$ MeV for the CDBonn interaction. Lower panels: absolute value of $\tilde{G}$ in the same conditions. The fully dressed pole is indicated by a cross, while the circle (square) show the position of the first (second) renormalization quasi-particle.

rise to a slightly different expression for the qp pole:

$$\varepsilon_{2'}(k) = \varepsilon_1(k) \tag{15}$$

$$\Gamma_{2'}(k) = \Gamma_1(k) \frac{1}{1 - \mathrm{Re}\tilde{\Sigma}'(\varepsilon_1(k))} \,. \tag{16}$$

As we shall see, this approximation is well justified only above k_F. Note that the previous expressions do not need any evaluation of self-energies in the complex plane. Access to real-energy self-energies, as those provided by Brueckner-Hartree-Fock, is enough to compute qp properties under the previous assumptions.

Once the qp spectrum and inverse lifetimes are known, one can go ahead and compute the mean-free path. Note, however, that this requires a consistent determination of ε, Γ and v, via Eq. (3). For the nuclear physics renormalization, Eqs. (15) and (16), the prefactor on the inverse lifetime is the inverse of the $\omega-$mass. The group velocity involves the full effective mass, $\frac{m^*}{m} = \frac{m_\omega}{m}\frac{m_k}{m}$. As a consequence, the mean-free path is only renormalized by the $k-$mass, $\lambda_{2'}(k) = \frac{m}{m_k}\lambda_0$, with respect to the uncorrected mean-free path, $\lambda_0(k) = k/[2m\,\mathrm{Im}\,\Sigma(k, \varepsilon_1(k)_+)]$. In this case, one can interpret the $k-$mass as a non-locality correction to the lowest order mean-free path. Within the nuclear physics community, this is a well-known correction that increases the mean-free path towards correct values [18, 19, 21].

3. Results

The upper panels of Figure 2 show the SCGF spectral function, as a function of energy, for three different characteristic momenta ($k = 0, k_F$ and $2k_F$). These have been obtained from a $T = 0$ self-energy based on the CDBonn interaction [27]. The lower panels give the absolute value of the continued propagator. One can clearly see, from the contour levels, that $\tilde{\mathcal{G}}$ develops a pole

in the lower half-plane. The location of this fully dressed pole is consistent with the numerical solution of Eq. (10), shown with a cross. Differences between this pole and the first or second renormalization predictions (corresponding to the circle and square, respectively) are visible at $k = 0$. At and above the Fermi surface, discrepancies disappear and the fully dressed pole coincides with the first and second renormalizations. This points towards a very soft dependence of Σ on the imaginary part of z for $k \geq k_F$. The contour lines, which are basically aligned along the imaginary axis, validate this picture. Let us highlight that, at the Fermi surface itself, the calculation yields a quasi-particle with zero width, providing a verification of Fermi liquid theory [34].

Nuclear many-body calculations are subject to uncertainties associated to the underlying NN interaction as well as to the approximation scheme itself. These uncertainties are explored in Fig. 3. The upper panel displays the mean-free path of a nucleon in homogeneous nuclear matter at a density of $\rho = 0.16$ fm^{-3} and zero temperature, obtained with a CDBonn self-energy supplemented with an Urbana-type 3BF [27]. As expected, we find that the largest discrepancies between different approximations occur for hole energies, below -20 MeV, in a region where λ is already relatively small. In contrast, above 50 MeV, all approximations give similar results, except for λ_0 (dashed line), which is not corrected for non-locality and thus should not be taken as a realistic prediction. $\lambda_{2'}$ (dashed-dotted line) is only somewhat larger than λ_0 because of the small m_k associated to the SCGF results. Note that the classical kinetic theory prediction, $\lambda \sim (\rho\sigma_{np})^{-1}$ (dotted lines), is well below all quantum in-medium mean-free paths. The latter flatten at high energies, and remain constant, at a value of around $4 - 5$ fm.

In contrast, the lower panel of Fig. 3 focuses on the NN interaction dependence of our results. All the mean-free paths here are obtained from the full pole in the complex plane. The $T = 0$ mean-free path with 3BF (solid line) is slightly larger than that obtained without 3BFs (dashed). We also study the importance of the two-body NN interactions at a temperature of $T = 5$ MeV. CDBonn results are shown in a dotted-dashed line, whereas Av18 results correspond to the double-dotted-dashed line. The largest differences are observed, again, at negative energies. Overall, the effect of changing two-body NN interactions is as large as that of switching 3BFs on or off. If one takes the spread between different lines as an estimate of theoretical uncertainties, these amount to less than 1 fm beyond 50 MeV. Note that this uncertainty is of the same order of that obtained from experimental estimates [37, 38] and that the theoretical prediction agrees well with those.

Fig. 4 focuses on the temperature and density dependence of the mean-free path in nuclear matter obtained from the full complex plane. This demonstrates that our method can be applied in a wide range of conditions. The upper panel displays the temperature dependence of λ for a typical density of a nuclear interior, $\rho = 0.16$ fm^{-3}. The effect of temperature is relevant in an area of about 20 MeV around the Fermi surface. By switching on temperature, the mean-free path at the Fermi surface immediately becomes finite due to thermal damping. The damping effect becomes larger as temperature increases and thus the value of λ at the Fermi surface, $\omega = \mu$, decreases as temperature increases. These results indicate that finite temperature calculations provide reliable estimates of zero-temperature properties away from the Fermi surface. In other words, thermal effects do not dominate the very high and low energy behaviour of the mean-free path.

The density dependence of the mean-free path, displayed in the lower panel of Fig. 4, is more pronounced at all energies. Near the Fermi surface, an increase in density leads to an increase of λ. This is expected based on degeneracy arguments. A system at larger density is more degenerate and thus closer to the zero-temperature case, where λ diverges at the Fermi surface. At an energy of around 70 MeV this tendency is reversed, though, and λ tends to decrease as the density grows. This behaviour is more intuitive, but it remains to be seen whether the $1/\rho$ dependence predicted by classical transport theory is valid in the fully correlated, quantum

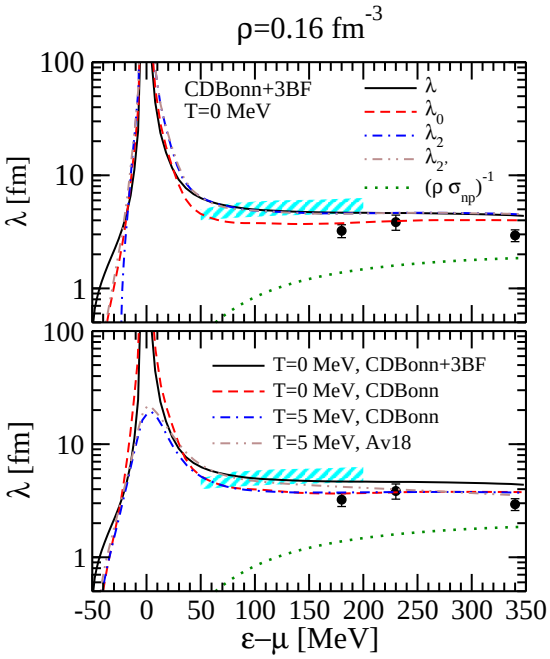

Figure 3. Mean-free path of a nucleon in nuclear matter as a function of energy. Upper panel: results obtained with a CDBonn+3BF self-energy at $T = 0$ MeV. The different approximations are commented on in the text. Lower panel: results obtained from the fully dressed pole for different NN forces and two different temperatures. The shaded band and solid dots correspond to the experimental results of Refs. [37, 38], respectively.

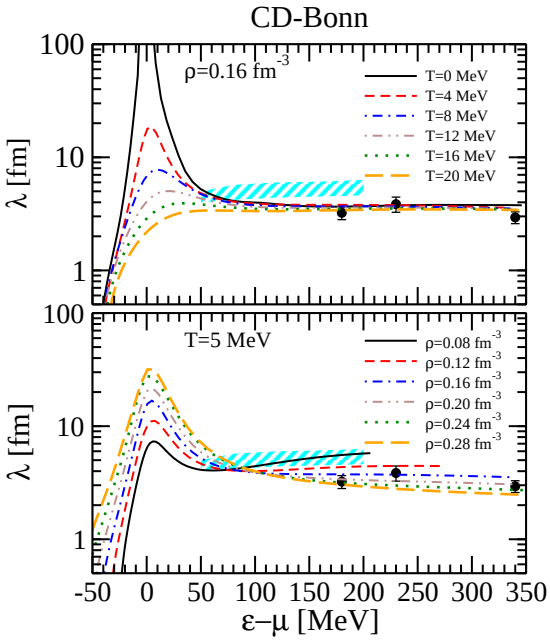

Figure 4. Mean-free path of a nucleon in nuclear matter as a function of energy. Upper panel: temperature dependence obtained with a CDBonn self-energy at a constant density of $\rho = 0.16$ fm^{-3}. Lower panel: density dependence obtained with a CDBonn self-energy at a constant temperature of $T = 4$ MeV.

case. The low density results cover the band of experimental data of Ref. [37], which has been extracted phenomenologically from finite nuclei. On average, these have a typical density which is lower than 0.16 fm^{-3} and thus this prediction meshes well with experimental estimates.

4. Conclusions and outline

We have devised a new method to obtain the mean-free path of a nucleon in the medium. The method involves the extension of Green's functions techniques into the complex plane and the determination of quasi-particle properties from a pole in the lower half-plane. Our approach provides a validation of previously used approximations by taking into account the full dependence on the imaginary part of the energy. In the nuclear medium, the calculation of the pole within this method provides similar mean-free paths as those obtained with earlier, cruder calculations. The renormalization induced by this procedure is specially relevant for hole properties. With all many-body corrections properly implemented, we obtain a mean-free path of around $4 - 5$ fm at saturation density and energies above 50 MeV.

The nucleon mean-free path lies at the heart of several theoretical and experimental considerations. Our future work will systematically assess the density, temperature and isospin asymmetry dependence of the mean-free path. In addition, we plan to compute other transport

coefficients using our ladder self-energies. Bulk viscosities are particularly important in the context of neutron stars. Ultimately, we aim at producing a consistent set of transport properties that can be validated thoroughly against pulsar observations.

Acknowledgments

This work has been supported by a Marie Curie Intra European Fellowship within the 7^{th} Framework programme, STFC grants ST/I005528/1 & ST/J000051/1 and the Espace de Structure Nucléaire Théorique (ESNT, CEA Saclay).

References

[1] Baldo M 1999 *Nuclear Methods and the Nuclear Equation of State* International Review of Nuclear Physics, Vol. 8 (World Scientific (Singapore))
[2] Lattimer J M and Prakash M 2007 *Phys. Rep.* **442** 109 (*Preprint* 0612440)
[3] Steiner A W, Lattimer J M and Brown E F 2010 *Astrophys. J.* **722** 33–54
[4] Özel F, Baym G and Güver T 2010 *Phys. Rev. D* **82** 101301
[5] Balescu R 1975 *Equilibrium and Nonequilibrium Statistical Mechanics* (*Wiley-Interscience publication* vol 76) (Wiley)
[6] Page D, Prakash M, Lattimer J and Steiner A 2011 *Phys. Rev. Lett.* **106** 081101
[7] Ho W, Andersson N and Haskell B 2011 *Phys. Rev. Lett.* **107** 101101
[8] Cutler C and Lindblom L 1987 *Astrophys. J.* **314** 234
[9] Wambach J, Ainsworth T and Pines D 1993 *Nucl. Phys. A* **555** 128–150
[10] Benhar O and Valli M 2007 *Phys. Rev. Lett.* **99** 232501
[11] Haskell B, Degenaar N and Ho W C G 2012 *MNRAS* **424** 93–103
[12] Benhar O, Polls A, Valli M and Vidaña I 2010 *Phys. Rev. C* **81**(2) 024305
[13] Abrikosov A A and Khalatnikov I M 329 *Rep. Prog. Phys.* **22** 329
[14] Economou E N 2006 *Green's Functions in Quantum Physics* 3rd ed Springer Series in Solid-State Sciences (Springer)
[15] Kadanoff L P and Baym G 1962 *Quantum Statistical Mechanics* First ed (New York: Benjamin)
[16] Mahan G D 1990 *Many-particle Physics* Second ed (NY: Plenum Press)
[17] Enss T, Haussmann R and Zwerger W 2011 *Ann. Phys.* **326** 770–796
[18] Negele J and Yazaki K 1981 *Phys. Rev. Lett.* **47** 71–74
[19] Fantoni S, Friman B L and Pandharipande V R 1981 *Phys. Lett. B* **104** 89–91
[20] Sinha B 1983 *Phys. Rev. Lett.* **50** 91–94
[21] Mahaux C 1983 *Phys. Rev. C* **28** 1848–1849
[22] Glavanakov I V 2004 *Physics of Atomic Nuclei* **67** 1580–1595
[23] Li G, Machleidt R and Zhuo Y 1993 *Phys. Rev. C* **48** 1062–1068
[24] Zuo W, Bombaci I and Lombardo U 1999 *Phys. Rev. C* **60** 024605
[25] Sammarruca F 2008 *Phys. Rev. C* **77** 047301
[26] Rios A, Polls A and Dickhoff W H 2009 *Phys. Rev. C* **79** 18 (*Preprint* 0904.2183)
[27] Somà V and Bożek P 2008 *Phys. Rev. C* **78** 054003
[28] Fradkin E S 1969 *Nucl. Phys.* **12** 466–484
[29] Engelsberg S and Schrieffer J R 1963 *Phys. Rev.* **131** 993–1008
[30] Eiguren A and Ambrosch-Draxl C 2008 *Phys. Rev. Lett.* **101** 036402
[31] Eiguren A, Ambrosch-Draxl C and Echenique P 2009 *Phys. Rev. B* **79** 245103
[32] Frick T and Müther H 2003 *Phys. Rev. C* **68** 034310
[33] Dickhoff W H and Barbieri C 2004 *Prog. Part. Nucl. Phys.* **52** 377–496
[34] Dickhoff W H and Van Neck D 2005 *Many-body theory exposed!* 1st ed (World Scientific)
[35] Abrikosov A A, Gorkov L P and Dzyaloshinskii I Y 1965 *Quantum Field Theoretical Methods in Statistical Physics* 2nd ed (Pergamon Press)
[36] Baym G and Mermin N D 1961 *J. Math. Phys.* **2** 232
[37] Nadasen A, Schwandt P, Singh P P, Jacobs W W, Bacher A D, Debevec P T, D K M and Meek J T 1981 *Phys. Rev. C* **23** 1023
[38] Renberg, P U and Measday, D F and Pepin, M and Schwaller, P and Favier, B and Richard-Serre C 1972 *Nucl. Phys. A* **183** 81